Impact of climate change on the transition of Neanderthals to modern humans in Europe

Michael Staubwasser[a,1], Virgil Drăgușin[b], Bogdan P. Onac[c,d], Sergey Assonov[a,e], Vasile Ersek[f], Dirk L. Hoffmann[g], and Daniel Veres[d]

[a]Institute of Geologie and Mineralogy, University of Cologne, 50674 Cologne, Germany; [b]Emil Racoviță Institute of Speleology, Romanian Academy, 010986 Bucharest, Romania; [c]School of Geosciences, University of South Florida, Tampa, FL 33620; [d]Emil Racoviță Institute of Speleology, Romanian Academy, 400006 Cluj-Napoca, Romania; [e]Terrestrial Environment Laboratory, Environmental Laboratories, Department of Nuclear Applications, International Atomic Energy Agency, 1400 Vienna, Austria; [f]Department of Geography and Environmental Sciences, Northumbria University, Newcastle upon Tyne NE1 8ST, United Kingdom; and [g]Department of Human Evolution, Max Planck Institute for Evolutionary Anthropology, 04103 Leipzig, Germany

Two speleothem stable isotope records from East-Central Europe demonstrate that Greenland Stadial 12 (GS12) and GS10—at 44.3–43.3 and 40.8–40.2 ka—were prominent intervals of cold and arid conditions. GS12, GS11, and GS10 are coeval with a regional pattern of culturally (near-)sterile layers within Europe's diachronous archeologic transition from Neanderthals to modern human Aurignacian. Sterile layers coeval with GS12 precede the Aurignacian throughout the middle and upper Danube region. In some records from the northern Iberian Peninsula, such layers are coeval with GS11 and separate the Châtelperronian from the Aurignacian. Sterile layers preceding the Aurignacian in the remaining Châtelperronian domain are coeval with GS10 and the previously reported 40.0- to 40.8-ka cal BP [calendar years before present (1950)] time range of Neanderthals' disappearance from most of Europe. This suggests that ecologic stress during stadial expansion of steppe landscape caused a diachronous pattern of depopulation of Neanderthals, which facilitated repopulation by modern humans who appear to have been better adapted to this environment. Consecutive depopulation–repopulation cycles during severe stadials of the middle pleniglacial may principally explain the repeated replacement of Europe's population and its genetic composition.

Central Europe | speleothems | millennial-scale climate cycles | stable isotopes | Middle—Upper Paleolithic transition

The replacement of Neanderthals by modern humans is recorded across Europe in a diachronous and culturally complex succession of distinct stone tool assemblages from the Middle–Upper Paleolithic transition (MUPT) roughly between 48 and 36 ka cal BP [calendar years before present (1950)] (1, 2). The succession often includes a regionally distinct "transitional" assemblage of local origin, or an intrusive Initial Upper Paleolithic assemblage between the Neanderthal Mousterian and modern human Aurignacian. The oldest anatomically modern human remains from Europe—found in East-Central Europe and radiocarbon dated to 40.6–38.6 ka cal BP (68% probability) toward the time of Neanderthals' disappearance from most of continental Europe—carry genetic evidence for species interbreeding four to six generations earlier (3–6). This individual, however, represents a population that did not contribute to the genome of modern humans present in glacial Europe after the MUPT (7), and the archeologic record provides no site with indication of local coexistence. Within a few millennia after the MUPT, at least two other genetically distinct modern human populations came to subsequently dominate Middle Pleniglacial Europe. During the entire interval, northern hemispheric climate went through several millennial-scale Dansgaard–Oeschger (DO) cold cycles (8, 9). A causality between climate change, the archeologic succession, and modern humans' genetic makeup has been tentatively suggested but not demonstrated (1, 2, 7). Below, we present the climatic history of continental Europe during the MUPT and derive the impact of climate change on MUPT demography, which may have led to the apparent repetitive genome turnover reported for Europe's human population during the middle pleniglacial.

The MUPT spans five DO cycles approximately between Greenland Interstadial 12 (GI12) and Greenland Stadial 8 (GS8) (9) for which climate change over continental Europe is poorly constrained. The paleoclimatic and environmental context is known with sufficient resolution and age-control only along the continent's western and southern fringe. In the Aegean and Black Sea region, records of sea surface temperature (10), coastal ice-rafted detritus (IRDc) (11), pollen assemblages (12–15), and stable isotopes in speleothems (16) suggest a DO-type response without the clear prominence of ice-rafting intervals (Heinrich stadials) seen in the Atlantic domain (17). Forest was generally more abundant in Europe during interstadials, while steppe landscape advanced during stadials (12). A taiga and tundra shrub/forest landscape covered the eastern European plains, with some loess deposition east of the Carpathians (12, 18, 19). The middle and lower Danube Plain was a steppe landscape with continuous loess deposition (20). A temperate open forest in the mountains of the southern Balkan passed into a xerophytic steppe toward the Aegean Sea (12, 13, 15). Boreal forest with birch and pine trees was present at 50° N in Western Europe (Eifel maar lakes) but began to degrade after GI12, ~44.5 ka cal BP (21). Two sparsely dated records from the Western Carpathians (Safarka, Jablunka) suggest a dense taiga forest landscape (14). For the upper Danube Plain, pollen (Füramoos) and loess/paleosol profiles (Willendorf II, Nussloch)

Significance

A causality between millennial-scale climate cycles and the replacement of Neanderthals by modern humans in Europe has tentatively been suggested. However, that replacement was diachronous and occurred over several such cycles. A poorly constrained continental paleoclimate framework has hindered identification of any inherent causality. Speleothems from the Carpathians reveal that, between 44,000 and 40,000 years ago, a sequence of stadials with severely cold and arid conditions caused successive regional Neanderthal depopulation intervals across Europe and facilitated staggered repopulation by modern humans. Repetitive depopulation–repopulation cycles may have facilitated multiple genetic turnover in Europe between 44,000 and 34,000 years ago.

suggest a cold steppe environment with few conifers during interstadials, and a tundra landscape with cryosoil formation during stadials (12, 22, 23). During GIs, a temperate forest-steppe prevailed west (marine records) and south of the Alps (Monticchio, Castiglione, and Lagaccione) (12). Dust deposition in the Eifel maar lakes and speleothem carbon isotopes from Villars Cave suggest increasing aridity in Western Europe across the MUPT (24, 25).

The MUPT Speleothem Paleoclimate Record of East-Central Europe

Here, we present two speleothem records from East-Central Europe (Romania). Stalagmite POM1 is from Ascunsă Cave (AC), South Carpathians, 50 km north of the Danube Valley at 1,050-m altitude (*SI Appendix*, Fig. S1). Stalagmite 1152 is from Tăuşoare Cave (TC), East Carpathians, at 950-m altitude, 2.5° north of the AC site. We dated the speleothems by U-Th and measured stable carbon and oxygen isotopes continuously at decadal resolution (*SI Appendix*, Fig. S2 and Table S1).

The AC speleothem $\delta^{13}C$ record reproduces the DO pacing of the Greenland ice core record during the MUPT (Fig. 1). The TC $\delta^{18}O$ record reproduces some aspects of the Greenland record. The climatic meaning of the AC $\delta^{13}C$ data may be constrained within context of other records from the region, particularly the
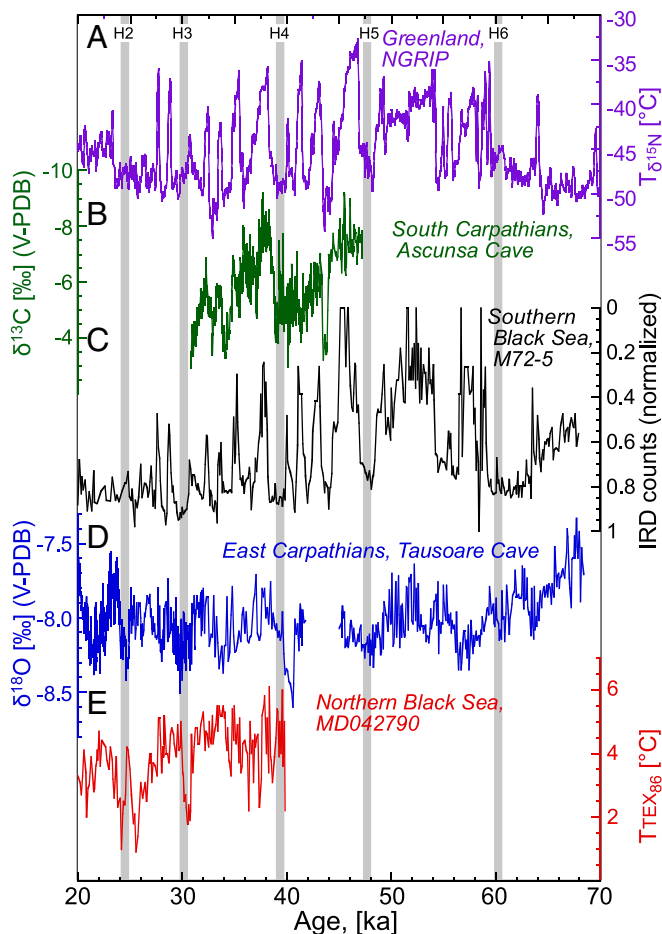

Fig. 1. (A) Greenland: North Greenland Ice Core Project (NGRIP) temperature (8). (B) South Carpathians: $\delta^{13}C$ of stalagmite POM1 from AC. (C) Southern Black Sea: coastal IRD abundance in core M72-5 (11). (D) East Carpathians: $\delta^{18}O$ of stalagmite 1152, TC. (E) Northern Black Sea: TEX$_{86}$ summer sea surface temperatures (33). The gray bars indicate Heinrich stadials. A map with locations of records is available in *SI Appendix*, Fig. S1.

Black Sea (Fig. 1). The coherency of the AC $\delta^{13}C$ record with southern Black Sea IRDc (11) implies that speleothem $\delta^{13}C$ responded to changes in the length of the sea ice and winter frost season. Chemically, speleothem $\delta^{13}C$ depends on the proportion of low $\delta^{13}C$ aqueous CO_2 derived from microbial respiration of soil organic matter above the cave (26). Extended frost and shorter plant growth seasons reduces the supply of fresh soil organic matter (SOM) and increases the proportion of CO_2 from old SOM in drip water, which has up to 8‰ higher $\delta^{13}C$ than fresh SOM under comparable conditions (27). Other potential controls are insufficient to explain the 6‰ amplitude of DO cycles in the speleothem. For example, the effect of a seasonally variable CO_2 degassing rate from drip water may add a kinetic fractionation effect on the $\delta^{13}C$ of precipitating speleothem calcite (28). However, recent monitoring showed that interannual variability in $\delta^{13}C$ of precipitating calcite in AC is less than 1.5‰ (29). Similarity between the AC $\delta^{13}C$ and $\delta^{18}O$ records is limited (*SI Appendix*, Fig. S3)—another qualitative argument against major kinetic isotope fractionation. Also, a compositional change in SOM $\delta^{13}C$ can be ruled out as variability in Central European paleosol profiles does not exceed 1‰ during the MUPT (30). Finally, variable moisture availability may have influenced soil formation above the cave and speleothem $\delta^{13}C$. The Danube loess record suggests such an interval of enhanced moisture availability after GI8 (20). The AC-speleothem $\delta^{18}O$ record does indeed suggest some change to that effect between GS8 and GI7, but the overall pacing across the MUPT resembles that of southeastern Mediterranean records and shows little coherency with DO cycles (see below). In general, soil formation intervals recorded by low values in AC-$\delta^{13}C$ are coeval with the range of ages obtained for paleosols in the upper Danube Willendorf II profile (Fig. 2). This suggests that the entire Danube region was inside the same climate zone and responded coherently to temperature change during DO cycles of the MUPT.

Little variance is observed in the East Carpathian TC $\delta^{13}C$ record (*SI Appendix*, Fig. S3). Here, pyrite weathering and enhanced limestone dissolution in the host rock obscures any potential influence on $\delta^{13}C$ from SOM (*SI Appendix*). That record is not considered in this study.

In general, speleothem $\delta^{18}O$ reflects a combination of calcite precipitation temperature—the annual average temperature inside the cave—and factors controlling $\delta^{18}O$ in drip water. Within a few days, water and dissolved CO_2 equilibrate isotopically in the aquifer above the cave, and drip water composition reflects regional hydroclimatology, that is, moisture source, rain-out history, local rain-out temperature, and the annual distribution of rainfall (26, 31). The AC $\delta^{18}O$ signal's overall amplitude is ~4‰. Such a large change is beyond reasonable temperature variability (28) and suggests a dominant influence of changes in hydrology on AC $\delta^{18}O$. The dissimilarity of AC $\delta^{18}O$ to the coherent $\delta^{13}C$ and Greenland temperature records (*SI Appendix*, Fig. S3) renders a temperature control of the AC $\delta^{18}O$ record unlikely. Hydroclimatic dominance on speleothem $\delta^{18}O$ is typical for the entire Eastern Mediterranean domain's Holocene record including at AC, which reflects significant variability in rainfall seasonality and moisture source proportions (31). The similar pacing between AC $\delta^{18}O$ and southeastern Mediterranean $\delta^{18}O$ record (*SI Appendix*, Fig. S4) may indicate that the underlying synoptic-scale mechanism was also active during MIS3.

The TC speleothem $\delta^{18}O$ record has an amplitude of ~1‰ and a different pacing compared with AC $\delta^{18}O$ (*SI Appendix*, Fig. S3). This suggests that the East Carpathians were in a different hydroclimatic regime during the MUPT. What defines the East Carpathian regime may be investigated by exploring the partial coherency between TC $\delta^{18}O$ and the other paleoclimate record. After ~60 ka, the $\delta^{18}O$ record shows low-amplitude variability with a few pronounced minima of ~0.5‰ that are coeval with some of the Greenland stadials (Fig. 1). These include GS3-H2, GS5-H3, and GS13-H5. Other minima just after 34 ka and at
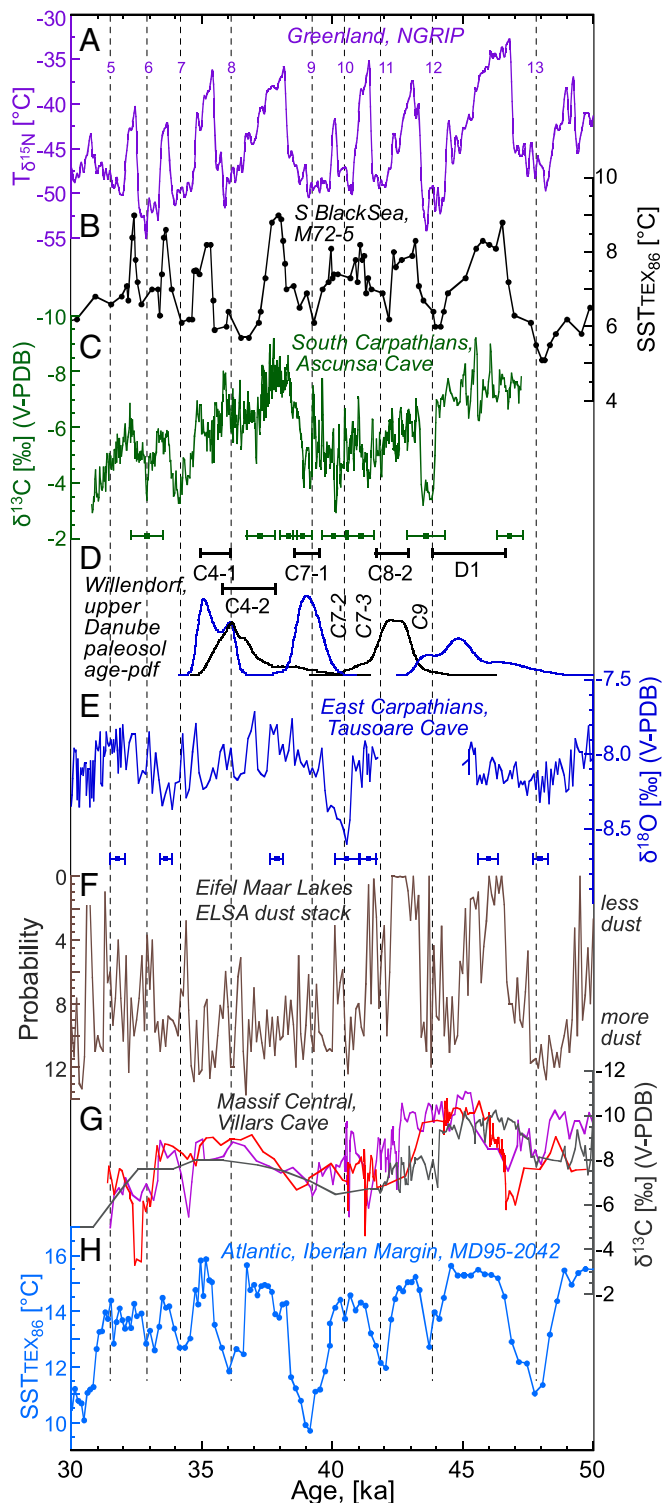
Fig. 2. (*A*) Greenland: NGRIP temperature (8). (*B*) Southern Black Sea: TEX$_{86}$ sea temperature core M72-5 (10). (*C*) South Carpathians: AC stalagmite POM1 δ^{13}C. (*D*) Upper Danube: Willendorf loess/paleosol profile, paleosol ages, age probability density functions (age-pdf), and stratigraphically constrained loess and gley horizons C7-2, C7-3, and C9 (22). (*E*) East Carpathians: TC stalagmite 1152 δ^{18}O. (*F*) Eifel maar lakes, ELSA dust stack. (*G*) Western Massive Central: Villars Cave stalagmites δ^{13}C (25). (*H*) Iberian Atlantic margin: TEX$_{86}$ sea surface temperature core MD95-2042 (17). Numbers indicate Greenland stadials at the end of the respective DO cycle. A map with locations of records is available in *SI Appendix*, Fig. S1.

41 ka correspond to GS7 and GS10 (Fig. 1). The latter lasted from 40.66 ± 0.47 ka$_{U-Th}$, P = 95%)—directly dated—to an interpolated end date of ~39.70 ± 0.43 ka (32). Although there may be a few centuries of overlap with GS9-H4, the measured age interval of 40.7–39.8 ka$_{U-Th}$, ±0.47 to ±0.3 uncertainty, matches GS10 (40.80–40.16 ka$_{GICC05}$) better than GS9-H4 (from 39.90 to 38.22 ka$_{GICC05}$) (9). A poorly resolved relative δ^{18}O maximum at 39.6 ± 0.4 ka$_{U-Th}$ and a subsequent broad relative δ^{18}O minimum in the TC record appear to be coeval with GI9 and GS9-H4, which apparently had a lesser impact on Central European climate. The TC δ^{18}O record thus responded to stadial cooling in the Atlantic but with a regionally controlled amplitude. Similarity with the northern Black Sea paleotemperature archive suggests this response is temperature driven (Fig. 1). For two reasons, TC δ^{18}O likely records the local summer temperature signal. First, the northern Black Sea record shows that summer sea surface temperature between 40 and 20 ka cal BP dropped by ~2 °C during stadials from a MIS3 average of 4–5 °C (33). Assuming published global empirical temperature relationships for cave calcite—Δδ^{18}O$_c$/ΔT = −0.18 (28)—and for rainwater in midlatitudes—where Δδ^{18}O$_w$/ΔT = 0.58 (34)—the 0.4–0.6‰ δ^{18}O amplitude in the TC speleothem would correspond to a comparable 1.0–1.5 °C temperature change. Second, palynologic, geomorphologic, and geochemical studies support this interpretation as follows. During the last glacial, the lowlands north of the East Carpathians were situated inside the tundra biome, where field evidence of ice wedges indicates permafrost conditions (35–37). Deep winter frost or even discontinuous permafrost is a likely scenario for the >1,000-m altitude of the ground above TC in the East Carpathians. At 20–40 ka, the average ground temperature of the northern Black Sea drainage basin—comprising the Danube, Dniestr, Dniepr, and Don Lowlands—was ~4 °C (38). Common adiabatic gradients of 6–10 °C per km of altitude imply that annual average ground temperatures above TC were lower than −2 °C. This suggests an alpine near-permafrost environment. Permafrost conditions may have been continuous during extreme stadials, thus preventing groundwater recharge to the cave and interrupting speleothem growth. During GS12—the coldest of all stadials in the Greenland record—the TC speleothem shows a hiatus coeval with the most pronounced δ^{13}C maximum in the AC speleothem further south. In the Willendorf II loess profile, this interval correlates with tundra gley horizon C9 with evidence of permafrost (22) (Fig. 2). C9 is constrained in time by paleosols C8-3 above and D1 underneath with dating ranges similar to GI11 and GI12, respectively. The Willendorf II profile is located at the same latitude as the TC speleothem, but only at 230-m altitude. Continuous permafrost conditions at 950-m altitude in the East Carpathians were thus likely during GS12. Seasonally permeable frost or discontinuous permafrost at other times would restrict speleothem growth to the summer season. Unlike the hydrologically dominated AC δ^{18}O record, TC δ^{18}O-only records regional summer temperature change.

Paleoclimatic Context of the Middle Pleniglacial in Europe

A reduction of forest and expansion of steppe biomes occurred during all stadials (12–15, 21), but climate records between the Atlantic and the Black Sea show a spatially heterogeneous response to DO cycles (Fig. 2). GS13-H5 is apparent in the TC speleothem δ^{18}O record but unlike in the Atlantic domain, its amplitude is small compared with subsequent stadials. Southern Black Sea IRDc data (Fig. 1) indicate less sea ice than during subsequent stadials despite apparent colder annual sea surface temperature (Fig. 2). This suggests a different seasonality with less severe winters. Thus, extreme cold was unlikely in East-Central Europe. The extreme aridity apparent in the Aegean region (13) may not have been as severe in the Balkan and Black Sea region (15, 16). GS12, from 43.4–44.3 ka$_{GICC05}$ or 43.3–44.0 ka$_{U-Th}$ (AC), is a very

prominent stadial in Greenland and Central Europe (Fig. 2), where permafrost changed the upper Danube lowland cold steppe into a tundra (see above). Malacological data from Willendorf II and the Eifel maar dust record suggests dryer conditions also in Western and Central Europe (22, 24) (Fig. 2). A cooling step likely occurred over Western Europe, supported by evidence of deep frost in the loess/paleosol record of northern France at ~43–44 ka cal BP (39). However, this stadial is less prominent in the Atlantic record (17). GS11 is present in all continental records, but not as pronounced as GS12. A common cooling trend superimposed over DO cycles 12–9 is apparent in all records (Fig. 2). GS10—from 40.1–40.9 ka$_{GICC05}$ and 39.7–40.7 ka$_{U-Th}$ (TC)—is a very prominent stadial over continental Europe, coeval with another cooling step in Western Europe (Fig. 2), but also a reduction in moisture and reduced speleothem growth (25). The first occurrence of loess in the Willendorf II profile (C7-2) around that time (22) and another strong dust peak in the Eifel maar record suggest stronger aridity than during GS12. Although present in all continental records, this stadial is unremarkable in the Atlantic and in the Black Sea (Fig. 2). However, annual sea surface temperature and winter coastal ice abundance in the Black Sea show conflicting results for GS10, which could again indicate a seasonality change. GS9-H4 is a long-lasting stadial that was less prominent in the Central European record but coeval with significant cooling and aridity in Western Europe (Fig. 2). Over the Atlantic and the Black Sea, GS9-H4 is a much more significant stadial. Subsequent GI8 is as warm as GI12 in Central Europe and the Black Sea region, with soil formation in the Danube region and East Carpathians (19, 20, 22), but colder in Western Europe and the Atlantic. Dust deposition in the Eifel maar records was also high during GI8, unlike GI13. The causes to this regionally heterogeneous response to DO climate cycles remain uncertain, but a variable influence of the Siberian high has been suggested (20).

Following the MUPT, GS8 from 36.6 to 35.5 ka$_{GICC05}$ and GI7 from 35.5 to 34.7 ka$_{GICC05}$ are difficult to separate from each other in the speleothem records. The Black Sea record shows severe cooling during GS8 (Fig. 2). The AC-δ^{18}O record suggests a significant fluctuation of the regional hydrologic condition during GS8 and GI7 in agreement with extended soil formation in the Danube Valley and the East Carpathians (19, 22). Higher moisture availability may have masked the temperature signal in AC-δ^{13}C. After GI7, a long-term cooling trend is superimposed on DO variability throughout Europe (Fig. 2), in many places coincident with a long drying trend (20, 25).

The Relationship Between Demography and Climate Change During GS12 and GS10

GS12 and GS10 stand out as the most significant stadials in Central and Western Europe during the MUPT with severe cold, aridity, retreat of woodland, and expansion of steppe biomes. The consequence for human populations present is reflected in regional population decline (40) and in hunted game species, which in Western Europe changed from bovine dominated to reindeer dominated (41). Climatic and environmental constraints may not per se prove causality between the archeologic succession, the rapid replacement of humans' genome, and climate change, respectively. However, they do allow testing such a scenario for chronological feasibility: The biome changes during GS12 and 10 likely forced the population in open woodland habitats throughout Europe to adapt their subsistence strategy or habitat track their preferred biome to survive. Where biomes changed significantly, adaptation may not have been possible. During GS12 and 10, the permafrost boundary encroached the upper Danube region and East Carpathians. Both speleothems presented here suggest a rapid onset of stadial cooling and aridity in continental Europe within a few decades (Fig. 2). Depopulation would have been the consequence of failure to adapt or migrate away in time.

A number of chronologically well-constrained archeologic records allow for testing directly the feasibility of a regional depopulation scenario during severe stadials. Culturally (nearly) sterile layers have been reported—directly ^{14}C dated or constrained by ^{14}C-dated cultural layers above and below—in some regions and mark an archeological hiatus of several centuries duration. While such layers in some places represent short-term sedimentologic events without apparent discontinuity of habitation (42), at many sites their time span is multicentennial. These layers mostly relate chronologically to the time of GS12 and GS10, and suggest regionally widespread depopulation for many centuries between two subsequent cultures. (Fig. 3) (SI Appendix, Table S2). During GS12, this is the case for sites from the upper and middle Danube region. At Geissenklösterle, near-sterile (geologic) layer 17 separates Mousterian and Aurignacian assemblages (43) and is directly dated to 44.4–42.7 and 43.5–42.0 ka cal BP by two samples, with a Bayesian model age of 42.9–42.1 ka cal BP (44). At Sesselfelsgrotte, sterile layer F is directly constrained by Mousterian layer G1, 45.8–44.3 ka cal BP, and the late Mousterian layer E3, 42.2–40.5 ka cal BP, both recalibrated (4, 45). At Willendorf II, sterile layer C9 and subsequent layer C8-3 containing Aurignacian artifacts are constrained between two dated paleosols D1 and C8-2 (Fig. 2) (22). Mousterian Neanderthal presence in the middle Danube region has been redated to until ~45 ka cal BP, just before GS12 (46). Two sites with Aurignacian finds, at Keilberg-Kirche (47), 43.6–41.7 ka cal BP recalibrated (4), and at Pes-kő Cave, 43.8–41.2 ka cal BP (48), immediately postdate GS12. These fit the scenario of a cultural hiatus but lack local constraint by older assemblages. All of the above suggest widespread Mousterian Neanderthal
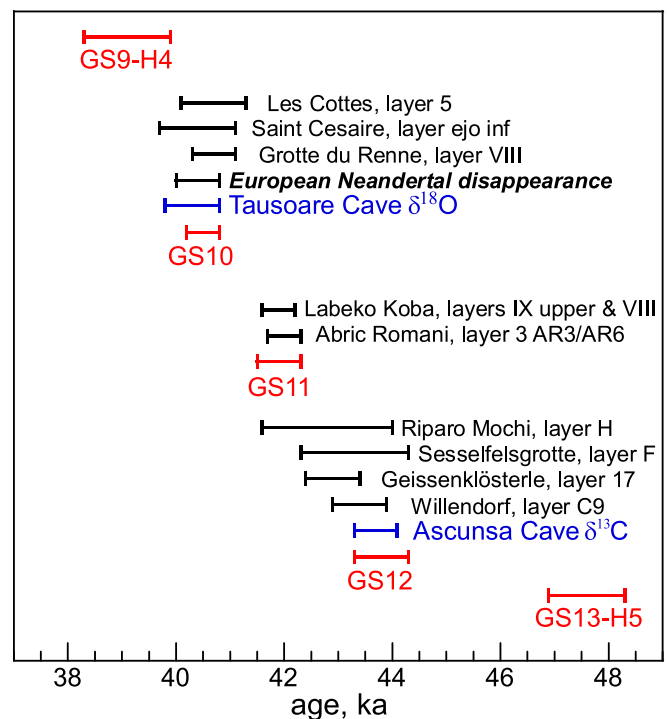

Fig. 3. The temporal pattern of Greenland stadials (red), prominent events in the Central European speleothem record (blue), and culturally (near-)sterile layers in archeologic records of Western and Central Europe (black). For stadials and speleothems, the bar shows the duration. For archeologic layers, the bar shows the 68% age interval (ka, cal BP) defined by the youngest date of the preceding layer and the oldest date of the succeeding layer. For details on archeologic radiocarbon chronologies, see SI Appendix, Table S2. A map with the locations of records is available in SI Appendix, Fig. S1.

depopulation of the upper and middle Danube Valley and—except for the tributary Altmühl Valley (49)—repopulation by Aurignacian after GS12.

Circumstantial evidence points to a similar impact of GS12 in northern Italy, where two sites, Riparo Mochi on the Ligurian Mediterranean coast—layer H—and at Grotta di Fumane in the Venetian Pre-Alps—layer A7—contain sterile layers probably coeval with GS12. However, reliable dating is only available for the base of the subsequent archeologic layer (50, 51) and age uncertainty is large (Fig. 3). A muted response to GS12 may be inferred for the site of Grotte Mandrin, Rhone Valley, where sterile layers separate strata C, B3, and B2 with post-Neronian-II artifacts (50). Layers B3–B1 of this latest regional Mousterian expression were dated in the range between 42.7 and 45.0 ka BP (6). These layers may indicate environmental change but do not appear to reflect longer breaks in the site's occupation. No such layers associated with GS12 are reported from archeologic sites further west. This suggests that the environmental impact of GS12 may have been less severe in Western Europe.

Sterile or near-sterile layers, or cultural hiatuses in the archeologic succession also occur around the time of GS10 (Fig. 3). This time is coeval with Neanderthals' disappearance from Western Europe (6). Sites include the Grotte-du-Renne—the low-density artifact layer VIII of intermittent Châtelperronian occupation (52); Les Cottés—sterile unit 5 (53); and Saint Césaire—layer Ejo inf (6). At Willendorf II, dated paleosols with lithic artifacts in C8 and C7 broadly constrain the sterile gley and loess horizons (C7-3 and C7-2) at that time (22) (Fig. 2). Subsequent archeologic layers are generally Aurignacian and document modern human expansion or reoccupation during GI9 and GI8 but under more arid conditions in Europe (Fig. 2).

A few archeologic profiles from around the Pyrenees—at Labeko Koba, Abric Romani, and possibly at Isturitz, but not at L'Arbreda (54–56)—contain sterile layers coeval with GS11 (Fig. 3). These represent a regional cultural hiatus between the Châtelperronian and the (Proto-)Aurignacian. However, apart from a long-term cooling and drying trend over Western Europe, an unambiguously dated climatic cold event cannot be detected in the present speleothem records for that time (Fig. 2).

A general case for likely adaptation of modern humans in response to climate change during the MUPT has already been made (48, 57, 58). Increasing cold and aridity around the onset of GS12 (Fig. 2) appears to mark transitions in the archeologic sequence attributable to Neanderthals that suggest some adaptation as well. GS12 is coeval with the transition from Mousterian to archaic Uluzzian, and then to evolved Uluzzian in northern Italy (59), and from Mousterian to Châtelperronian in Western Europe (53). However, late Neanderthals may have had a less diverse diet than modern humans (60). In open grasslands, Neanderthals' exclusive diet was meat from terrestrial animals, whereas modern human Aurignacian also exploited plant and aquatic foods (60, 61). The frequently observed cultural hiatuses, however, do not suggest a direct competitive displacement of Neanderthals, but rather a higher vulnerability to rapid environmental change and ecologic stress in the open landscape during cold and arid GS12–GS10. While Neanderthals did not survive GS12 in most of the Danube steppe and tundra, modern humans may have been more capable to adapt and habitat track the expanding steppe in Central Europe. GS10 likely caused a repeat of that process in Western Europe.

A depopulation scenario was suggested for GS13-H5 as a trigger for the first intrusion of modern humans into Europe, represented by the Bohunician stone tool assemblage in Moravia (Central Europe) and further east (13, 62). Because a potential cultural hiatus is difficult to prove in the archeologic record of Moravia at given accuracy and precision of applied radiometric dating methods (63), this scenario may not currently be tested. There is also not as strong a climatic evidence in support. Cooling likely was less severe in East-Central Europe compared with subsequent stadials (see above). Severe aridity was apparent between the northern Aegean coastal region and the Levant (13, 64) but not over the Balkan (15), the Adriatic and the Black Sea regions (16, 65), or Central-East Europe.

The Moravian record suggests contemporaneity of modern humans—the Bohunician—and Neanderthals—the Szeletian—at close geographic proximity during GI12 and perhaps later but with some chronologic uncertainty (63, 66). During GI11-10, the situation is comparable for the Aurignacian and Mousterian on the upper Danube—at Keilberg-Kirche and Sesselfelsgrotte (see above)—and for Aurignacian and Szeletian on the middle Danube—at Pes-kő Cave and Szeleta Cave (42, 67) (*SI Appendix,* Fig. S1). Here, however, the interbreeding between species only six generations before the lifetime of the Oase Cave modern human specimen in that time range (5) principally confirms true contemporaneity along the northern fringe of the steppe landscape in the Danube Valley. Nonetheless, in the subsequent ~6 millennia after GS10, the modern human genome in Europe was replaced twice with a different genetic lineage harboring a much older Neanderthal ancestry (7). One modern European genetic branch found inside Goyet Cave (Belgium), was attributed to the late Aurignacian and dated to ~35 ka cal BP—coeval with GI7. This interval of modern human repopulation may have followed the extended cold interval from GS10 to GS9-H4, over 4,000 y long and only interrupted briefly by the 250-y-long GI9 (Fig. 2). A different genetic branch then dominated Europe after ~34 ka cal BP—coeval to the end of the severe and 1,000-y-long GS7 (Fig. 2). This lineage was attributed to the Gravettian (7), who repopulated Europe during yet another time of low population density (68). The discussion above lays out a general scenario of depopulation–repopulation cycles associated with steppe landscape expansion following extreme or long stadials. The comparable timing of stadials and population changes seen in the archeologic and genetic record suggests that millennial-scale climate cycles may have been the pacesetter for Europe's demographic history during the Middle Pleniglacial.

1. Hoffecker JF (2009) Out of Africa: Modern human origins special feature: The spread of modern humans in Europe. *Proc Natl Acad Sci USA* 106:16040–16045.
2. Hublin J-J (2015) The modern human colonization of western Eurasia: When and where? *Quat Sci Rev* 118:194–210.
3. Trinkaus E, et al. (2003) An early modern human from the Peştera cu Oase, Romania. *Proc Natl Acad Sci USA* 100:11231–11236.
4. Reimer PJ, et al. (2013) Intcal13 and Marine13 radiocarbon age calibration curves 0–50,000 years cal Bp. *Radiocarbon* 55:1869–1887.
5. Fu Q, et al. (2015) An early modern human from Romania with a recent Neanderthal ancestor. *Nature* 524:216–219.
6. Higham T, et al. (2014) The timing and spatiotemporal patterning of Neanderthal disappearance. *Nature* 512:306–309.
7. Fu Q, et al. (2016) The genetic history of ice age Europe. *Nature* 534:200–205.
8. Kindler P, et al. (2014) Temperature reconstruction from 10 to 120 kyr b2k from the NGRIP ice core. *Clim Past* 10:887–902.
9. Rasmussen SO, et al. (2014) A stratigraphic framework for abrupt climatic changes during the last glacial period based on three synchronized Greenland ice-core records: Refining and extending the INTIMATE event stratigraphy. *Quat Sci Rev* 106:14–28.
10. Wegwerth A, et al. (2015) Black Sea temperature response to glacial millennial-scale climate variability: Black Sea temperature and DO cycles. *Geophys Res Lett* 42:8147–8154.
11. Nowaczyk NR, et al. (2012) Dynamics of the Laschamp geomagnetic excursion from Black Sea sediments. *Earth Planet Sci Lett* 351-352:54–69.
12. Fletcher WJ, et al. (2010) Millennial-scale variability during the last glacial in vegetation records from Europe. *Quat Sci Rev* 29:2839–2864.

13. Müller UC, et al. (2011) The role of climate in the spread of modern humans into Europe. *Quat Sci Rev* 30:273–279.

14. Feurdean A, et al. (2014) Climate variability and associated vegetation response throughout Central and Eastern Europe (CEE) between 60 and 8 ka. *Quat Sci Rev* 106: 206–224.

15. Panagiotopoulos K, et al. (2014) Climate variability over the last 92 ka in SW Balkans from analysis of sediments from Lake Prespa. *Clim Past* 10:643–660.

16. Fleitmann D, et al. (2009) Timing and climatic impact of Greenland interstadials recorded in stalagmites from northern Turkey. *Geophys Res Lett* 36:L19707.

17. Darfeuil S, et al. (2017) Sea surface temperature reconstructions over the last 70kyr off Portugal: Biomarker data and regional modeling. *Paleoceanography* 31:40–65.

18. Bokhorst MP, et al. (2011) Atmospheric circulation patterns in central and eastern Europe during the Weichselian Pleniglacial inferred from loess grain-size records. *Quat Int* 234:62–74.

19. Haesaerts P, et al. (2010) Charcoal and wood remains for radiocarbon dating upper Pleistocene loess sequences in eastern Europe and central Siberia. *Palaeogeogr Palaeoclimatol Palaeoecol* 291:106–127.

20. Obreht I, et al. (2017) Shift of large-scale atmospheric systems over Europe during late MIS 3 and implications for modern human dispersal. *Sci Rep* 7:5848.

21. Sirocko F, et al. (2016) The ELSA-vegetation-stack: Reconstruction of landscape evolution zones (LEZ) from laminated Eifel maar sediments of the last 60,000 years. *Global Planet Change* 142:108–135.

22. Nigst PR, et al. (2014) Early modern human settlement of Europe north of the Alps occurred 43,500 years ago in a cold steppe-type environment. *Proc Natl Acad Sci USA* 111:14394–14399.

23. Moine O, et al. (2017) The impact of last glacial climate variability in west-European loess revealed by radiocarbon dating of fossil earthworm granules. *Proc Natl Acad Sci USA* 114:6209–6214.

24. Sirocko F, et al. (2013) Multi-proxy dating of Holocene maar lakes and Pleistocene dry maar sediments in the Eifel, Germany. *Quat Sci Rev* 62:56–76.

25. Genty D, et al. (2010) Isotopic characterization of rapid climatic events during OIS3 and OIS4 in Villars Cave stalagmites (SW-France) and correlation with Atlantic and Mediterranean pollen records. *Quat Sci Rev* 29:2799–2820.

26. Dreybrodt W, Scholz D (2011) Climatic dependence of stable carbon and oxygen isotope signals recorded in speleothems: From soil water to speleothem calcite. *Geochim Cosmochim Acta* 75:734–752.

27. Wang G, Jia Y, Li W (2015) Effects of environmental and biotic factors on carbon isotopic fractionation during decomposition of soil organic matter. *Sci Rep* 5:11043.

28. Tremaine DM, Froelich PN, Wang Y (2011) Speleothem calcite farmed in situ: Modern calibration of δ^{18}O and δ^{13}C paleoclimate proxies in a continuously-monitored natural cave system. *Geochim Cosmochim Acta* 75:4929–4950.

29. Drăgușin V, et al. (2017) Transfer of environmental signals from the surface to the underground at Ascunsă Cave, Romania. *Hydrol Earth Syst Sci* 21:5357–5373.

30. Hatté C, et al. (2013) Excursions to C4 vegetation recorded in the upper Pleistocene loess of surduk (Northern Serbia): An organic isotope geochemistry study. *Clim Past* 9: 1001–1014.

31. Drăgușin V, et al. (2014) Constraining Holocene hydrological changes in the Carpathian–Balkan region using speleothem ^{18}O and pollen-based temperature reconstructions. *Clim Past* 10:1363–1380.

32. Scholz D, Hoffmann DL (2011) StalAge–An algorithm designed for construction of speleothem age models. *Quat Geochronol* 6:369–382.

33. Ménot G, Bard E (2012) A precise search for drastic temperature shifts of the past 40,000 years in southeastern Europe: Abrupt SST event in southeastern Europe. *Paleoceanography,* 27:PA2210.

34. Rozanski K, Araguas-Araguas L, Gonfiantini R (1993) Isotopic patterns in modern global precipitation. *Climate Change in Continental Isotope Records*, Geophysical Monograph, eds Swart PK, et al. (American Geophysical Union, Washington, DC), pp 1–36.

35. Huntley B, et al. (2003) European vegetation during marine oxygen isotope Stage-3. *Quat Res* 59:195–212.

36. van Huissteden K, Vandenberghe J, Pollard D (2003) Palaeotemperature reconstructions of the European permafrost zone during marine oxygen isotope stage 3 compared with climate model results. *J Quat Sci* 18:453–464.

37. Vandenberghe J, et al. (2014) The last permafrost maximum (LPM) map of the northern hemisphere: Permafrost extent and mean annual air temperatures, 25–17 ka BP. *Boreas* 43:652–666.

38. Sanchi L, Menot G, Bard E (2014) Insights into continental temperatures in the northwestern Black Sea area during the last glacial period using branched tetraether lipids. *Quat Sci Rev* 84:98–108.

39. Antoine P, et al. (2016) Upper Pleistocene loess-palaeosol records from northern France in the european context: Environmental background and dating of the middle palaeolithic. *Quat Int* 411:4–24.

40. Morin E (2008) Evidence for declines in human population densities during the early Upper Paleolithic in western Europe. *Proc Natl Acad Sci USA* 105:48–53.

41. Discamps E, Jaubert J, Bachellerie F (2011) Human choices and environmental constraints: Deciphering the variability of large game procurement: From mousterian to Aurignacian times (MIS 5-3) in southwestern France. *Quat Sci Rev* 30:2755–2775.

42. Vandevelde S, Brochier JÉ, Petit C, Slimak L (2017) Establishment of occupation chronicles in Grotte Mandrin using sooted concretions: Rethinking the middle to upper paleolithic transition. *J Hum Evol* 112:70–78.

43. Conard NJ, Bolus M (2003) Radiocarbon dating the appearance of modern humans and timing of cultural innovations in Europe: New results and new challenges. *J Hum Evol* 44:331–371.

44. Higham T, et al. (2012) Testing models for the beginnings of the Aurignacian and the advent of figurative art and music: The radiocarbon chronology of Geißenklösterle. *J Hum Evol* 62:664–676.

45. Böhner U (2008) *Sesselfelsgrotte IV—Die Schicht E3 der Sesselfelsgrotte und die Funde am Abri Schulerloch* (Franz Steiner Verlag Stuttgart, Stuttgart, Germany).

46. Devièse T, et al. (2017) Direct dating of Neanderthal remains from the site of Vindija cave and implications for the middle to upper paleolithic transition. *Proc Natl Acad Sci USA* 114:10606–10611.

47. Uthmeyer T (1996) Ein bemerkenswert frühes Inventar des Aurignacien von der Freilandfundstelle "Keilberg-Kirche" bei Regensburg. *Archaeologisches Korrespondenzblatt* 26:233–248.

48. Davies W, et al. (2015) Evaluating the transitional mosaic: Frameworks of change from Neanderthals to *Homo sapiens* in eastern Europe. *Quat Sci Rev* 118:211–242.

49. Richter J (2016) Leave at the height of the party: A critical review of the middle paleolithic in western central Europe from its beginnings to its rapid decline. *Quat Int* 411:107–128.

50. Douka K, Grimaldi S, Boschian G, del Lucchese A, Higham TF (2012) A new chronostratigraphic framework for the upper palaeolithic of Riparo Mochi (Italy). *J Hum Evol* 62:286–299.

51. Higham T, et al. (2009) Problems with radiocarbon dating the middle to upper palaeolithic transition in Italy. *Quat Sci Rev* 28:1257–1267.

52. Hublin J-J, et al. (2012) Radiocarbon dates from the Grotte du Renne and Saint-Césaire support a Neandertal origin for the Châtelperronian. *Proc Natl Acad Sci USA* 109:18743–18748.

53. Talamo S, et al. (2012) A radiocarbon chronology for the complete middle to upper Palaeolithic transitional sequence of Les Cottés (France). *J Archaeol Sci* 39:175–183.

54. Barshay-Szmidt C, et al. (2018) Radiocarbon dating the Aurignacian sequence at Isturitz (France): Implications for the timing and development of the proto-aurignacian and early Aurignacian in western Europe. *J Archaeol Sci Rep* 17:809–838.

55. Wood RE, et al. (2014) The chronology of the earliest upper palaeolithic in northern Iberia: New insights from L'Arbreda, Labeko Koba and La Viña. *J Hum Evol* 69:91–109.

56. Camps M, Higham T (2012) Chronology of the Middle to Upper Palaeolithic transition at Abric Romaní, Catalunya. *J Hum Evol* 62:89–103.

57. Banks WE, d'Errico F, Zilhão J (2013) Human-climate interaction during the early upper palaeolithic: Testing the hypothesis of an adaptive shift between the proto-Aurignacian and the early Aurignacian. *J Hum Evol* 64:39–55.

58. Riel-Salvatore J, Popescu G, Barton CM (2008) Standing at the gates of Europe: Human behavior and biogeography in the southern Carpathians during the late Pleistocene. *J Anthropol Archaeol* 27:399–417.

59. Douka K, et al. (2014) On the chronology of the Uluzzian. *J Hum Evol* 68:1–13.

60. Richards MP, Trinkaus E (2009) Out of Africa: Modern human origins special feature: Isotopic evidence for the diets of European Neanderthals and early modern humans. *Proc Natl Acad Sci USA* 106:16034–16039.

61. El Zaatari S, Grine FE, Ungar PS, Hublin J-J (2016) Neandertal versus modern human dietary responses to climatic fluctuations. *PLoS One* 11:e0153277.

62. Hoffecker JF (2011) The early upper Paleolithic of eastern Europe reconsidered. *Evol Anthropol* 20:24–39.

63. Skrdla P (2017) Middle to Upper Paleolithic transition in Moravia: New sites, new dates, new ideas. *Quat Int* 450:116–125.

64. Torfstein A, Goldstein SL, Stein M, Enzel Y (2013) Impacts of abrupt climate changes in the levant from last glacial dead sea levels. *Quat Sci Rev* 69:1–7.

65. Tzedakis PC, et al. (2004) Ecological thresholds and patterns of millennial-scale climate variability: The response of vegetation in Greece during the last glacial period. *Geology* 32:109–112.

66. Nigst PR (2014) First modern human occupation of Europe: The middle Danube region as a case study. *Living in the Landscape: Essays in Honour of Graeme Barker*, McDonald Institute Monographs, eds Boyle K, Rabett RJ, Hunt CO (McDonald Institute for Archaeological Research, University of Cambridge, Cambridge, UK), pp 35–47.

67. Hauck TC, et al. (2016) Neanderthals or early modern humans? A revised C-14 chronology and geoarcheological study of the Szeletian sequence in Szeleta Cave (Kom. Borsod-Abauj-Zemplen) in Hungary. *Archaeologisches Korrespondenzblatt* 46: 271–290.

68. Bicho N, Cascalheira J, Gonçalves C (2017) Early Upper Paleolithic colonization across Europe: Time and mode of the Gravettian diffusion. *PLoS One* 12:e0178506.

EARTH, ATMOSPHERIC, AND PLANETARY SCIENCES

ANTHROPOLOGY